# 3D inversion of towed streamer EM data – A model study of the Harding field and comparison to 3D CSEM inversion

*Michael S. Zhdanov, TechnoImaging, Bruce A. Hobbs, PGS, Masashi Endo*, Leif H. Cox, Noel Black, Alexander V. Gribenko, Martin Čuma, Glenn A. Wilson, TechnoImaging, and Ed Morris, PGS*

**Summary**

A towed streamer electromagnetic (EM) system capable of simultaneous seismic and CSEM data acquisition has been developed and tested in the North Sea. The towed EM data are processed and delivered as a time-domain impulse response. In this paper, we use 3D modeling and inversion to investigate the ability of the towed EM system to detect and characterize the Harding field, a typical North Sea-type target. The 3D model of the Harding field itself was constructed from dynamic reservoir simulations. We have compared our 3D inversion of time-domain towed streamer EM data with 3D inversion of conventional frequency-domain CSEM data. We observe similarities in the recovered models. Obviating the need for ocean bottom receivers, the towed-streamer EM system enables CSEM data to be acquired simultaneously with seismic over very large areas in frontier and mature basins for higher production rates and relatively lower cost than conventional CSEM.

**Introduction**

Controlled-source electromagnetic (CSEM) surveys are used for de-risking exploration and appraisal with direct hydrocarbon indication, where the survey designs have been characterized by arrays of fixed ocean-bottom receivers and towed transmitters (e.g., Hesthammer et al., 2010). However, relatively high acquisition costs have represented a significant obstacle to widespread adoption of conventional CSEM technology. To this end, a towed-streamer system capable of simultaneous seismic and CSEM data acquisition has recently been developed (Mattsson et al., 2010) (Figure 1). This moving platform geometry enables CSEM to be acquired over very large areas in both frontier and mature basins for higher production rates and relatively lower cost compared to conventional CSEM. However, 3D inversion of this data poses a significant challenge because of the scale of the surveys (1000s of square km), the number of transmitters and receivers, and the required model resolution (~100 m).

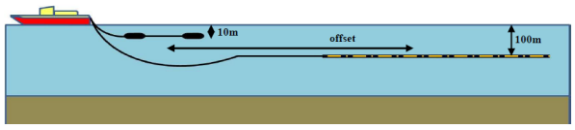


**Figure 1.** *Typical inline towing configuration of sources and receivers for towed EM system.*

To realize 3D inversion of entire towed streamer EM surveys, we introduce a moving footprint approach. The size of the towed EM system's footprint is significantly less than the size of the survey area, yet contains all the system's sensitivity. The sensitivities for the entire 3D earth model are then constructed as the superposition of footprints from all transmitter-receiver pairs over the 3D earth model (Figure 2). This concept has been successfully developed for 3D airborne EM (AEM) inversion (e.g., Cox et al., 2010), as well as 3D MT inversion (Zhdanov et al., 2011). It follows that memory and computational requirements can be reduced by several orders of magnitude, making large-scale 3D EM inversion a tractable problem. Moreover, our implementation can be used for both time- and frequency-domain towed EM data and has been parallelized with near-linear scaling. We demonstrate our approach with the 3D inversion of synthetic towed EM data from Harding field in the North Sea, and compare our results to those obtained from conventional frequency-domain CSEM surveys over the same target.

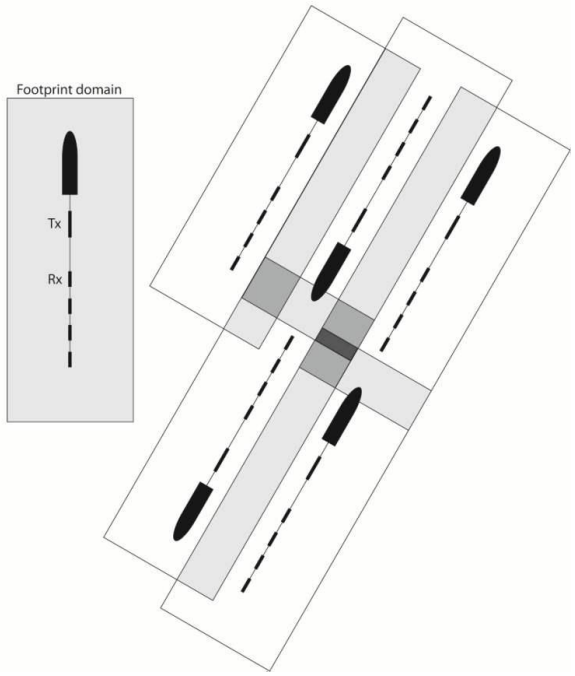


**Figure 2.** *Plan view of multiple towed EM footprints superimposed over the same 3D earth model. Darker shading indicates a higher overlap of different footprint domains.*

# 3D inversion of towed EM data

## Inversion methodology

Re-weighted regularized conjugate gradient (RRCG) methods are the only practical approach to solving large-scale 3D EM inversion problems as they update the model conductivities, $\boldsymbol{\sigma}$, with an iterative scheme akin to the following:

$$\boldsymbol{\sigma}_{i+1} = \boldsymbol{\sigma}_i + \Delta\boldsymbol{\sigma}_i = \boldsymbol{\sigma}_i + k_i \mathbf{F}_i^{\mathrm{T}} \mathbf{r}_i,$$

where $k_i$ is a step length, $\mathbf{F}_i^{\mathrm{T}}$ is the transpose of the $N_d \times N_m$ Fréchet matrix $\mathbf{F}_i$ of normalized sensitivities, and $\mathbf{r}_i$ is the $N_d$ length vector of the residual fields between the observed and predicted data on the $i^{\mathrm{th}}$ iteration (Zhdanov, 2002). Data and model weights which re-weight the inverse problem in logarithmic space are introduced in order to reduce the dynamic range of both the data and conductivity. The inversion iterates until the residual error reaches a preset threshold, the decrease in error between multiple iterations becomes less than a preset threshold, or a maximum number of iterations is reached.

Traditional regularized inversion methods recover smooth solutions, and thus have difficulties recovering sharp boundaries between different geological formations without having a priori information about those boundaries enforced. Focusing regularization makes it possible to recover subsurface models with sharper resistivity contrasts and boundaries than can be obtained with smooth stabilizers, and do not require those boundaries to be enforced a priori (e.g., Zhdanov et al., 2010).

At each iteration, computing the sensitivities for an entire towed EM survey and multiplying the transpose of the Fréchet matrix by the residual is not trivial. Even for a "small" towed EM survey, an inversion domain of 2,500,000 model cells and 40,000 data points may be reasonably expected. This would result in a Fréchet matrix requiring approximately 1.6 TB in storage, which is impractical to calculate and store, let alone manipulate or decompose at successive iterations. With a moving footprint approach, we can dramatically reduce our memory requirements, as not every transmitter or receiver has sensitivity to every cell of the entire 3D earth model. We note that our moving footprint inversion methodology is independent as to whether the towed EM data is delivered in time or frequency domains.

## Time-domain EM modeling

Time-domain EM modeling can be accomplished either by direct, time-domain solutions or by Fourier transformation of frequency-domain solutions. The latter offers three distinct advantages. First, the effects of frequency-dependent conductivity, such as induced polarization, can be modeled. Second, artificial dispersion effects that arise in direct time-domain solutions are avoided. Third, matrix equations with multiple terms on the right hand side can be rapidly solved with iterative solutions.

Our 3D frequency-domain modeling is based on an implementation of the contraction integral equation method that exploits the Toeplitz structure of the large, dense matrix system in order to solve multiple right-hand side source vectors using an iterative method with fast matrix-vector multiplications provided by a 2D FFT convolution (Hursán and Zhdanov, 2002). This implementation reduces storage and complexity, and lends itself well to large-scale parallelization. Once the Green's tensors have been pre-computed, they are stored and re-used, further reducing run time. In a moving footprint inversion, there is no need to calculate the Green's body-to-receiver tensors and background fields for those cells beyond the footprint of a given transmitter-receiver pair. Moreover, since the background model is horizontally layered, the body-body Green's tensors are horizontally invariant. The electric Green's tensors are identical for each footprint domain and are then translated over the entire inversion domain, speeding up the computation and increasing memory efficiency.

For calculating time-domain responses and sensitivities, the frequency-domain responses and sensitivities are computed at ten frequencies per decade logarithmically spaced from 1 mHz to 10 Hz. The imaginary components are splined and extrapolated back to zero frequency. The time-domain step response is calculated from a cosine transform evaluated using digital filters. The time-domain impulse response can be obtained from differentiation of the spline coefficients of the step response.

## Model study – Harding field, North Sea

Harding is a medium-sized oil and gas field covering approximately 20 km$^2$ that is located in block 9/23B in the UK sector of the North Sea, about 320 km northeast of Aberdeen (Figure 3). The field has a high net-to-gross, high quality, Eocene Balder sandstone reservoir about 1700 m below the seafloor in a 110 m water column. With 300 Mboe initially in place, production commenced in 1996 from the Harding Central and South reservoirs. Since then, two further reservoirs have been developed; Harding South East, and by extended reach drilling, Harding North. The reservoirs contain gas, and this has been injected back into a gas cap for later production. Oil production is now in decline, with current production of approximately 10,000 bpd with increasing water cut. The remaining hydrocarbon column consists of a gas cap about 100 m thick, and a thin oil rim about 20 m thick (Ziolkowski et al., 2010).

## 3D inversion of towed EM data

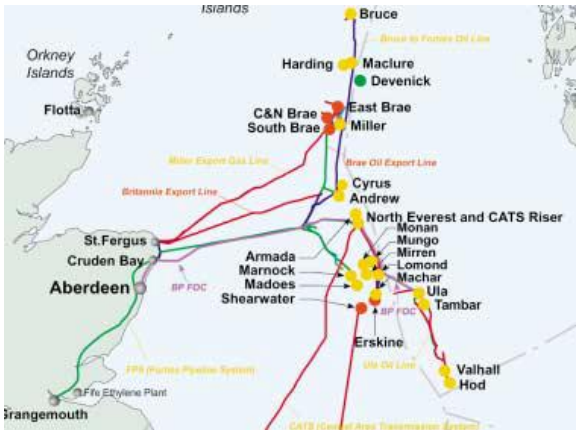


**Figure 3.** *Location of Harding field (courtesy of BP).*

The Harding Central dynamic reservoir models are populated by porosity and fluid saturations. Core analysis shows the Balder sands at Harding to be clean, so Archie's law is appropriate to relate the various petrophysical properties to an isotropic resistivity. Resistivity logs from well 9/23b-7 showed resistivities greater than 1200 ohm-m through the dry gas intervals. In actuality, some intervals may exceed resistivities of 1200 ohm-m, but resistive limits of EM responses means that their values are indiscernible from EM data. The 3D model consisted of a 110 m 0.3 ohm-m water column overlying an otherwise homogeneous half-space of 1.0 ohm-m in which the Harding Central reservoir model (Figure 4) was embedded (Ziolkowski et al., 2010).

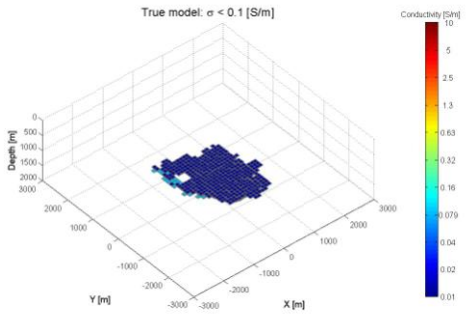


**Figure 4.** *3D perspective view of the Harding Central reservoir, with conductivity values less than 0.1 S/m (10 ohm-m) shown.*

The towed EM survey consisted of six survey lines; three oriented north-south, and three-oriented east-west. The line spacing was 1 km. Each line contained 31 transmitter-receiver pairs (198 total) spaced 200 m apart. The towed EM system consisted of a 300 m long electric bipole transmitter towed 10 m below the sea surface, and inline electric field receivers towed 50 m below the sea surface at offsets of 1325 m, 1850 m, 2025 m, and 2545 m. Data were simulated for the impulse response. For inversion, data were above threshold for the respective noise floor.

The CSEM survey consisted of six survey lines, three oriented north-south, and three oriented east-west. The CSEM survey was actually collocated with the towed EM survey. The line spacing was 1 km. Each line contained 11 receivers spaced 500 m apart, giving a total of 66 receivers. Data were simulated to offsets of 5500 m for inline and vertical electric fields and transverse magnetic fields at frequencies of 0.10, 0.25, 0.50 and 0.75 Hz. For inversion, data were above threshold for the respective noise floors.

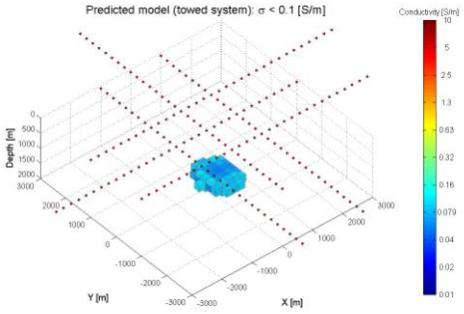


**Figure 5.** *3D perspective view of the Harding Central reservoir recovered from 3D towed EM inversion, with conductivity values less than 0.1 S/m (10 ohm-m) shown. The towed EM transmitter positions are superimposed on this image. The inversion was for the step response of the inline electric fields only.*

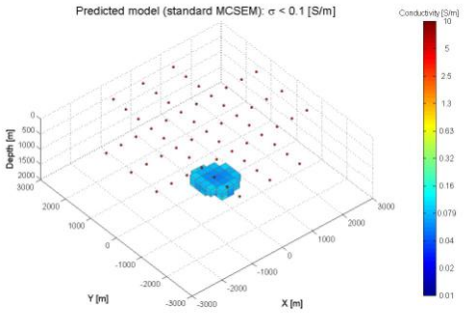


**Figure 6.** *3D perspective view of the Harding Central reservoir recovered from 3D CSEM inversion, with conductivity values less than 0.1 S/m (10 ohm-m) shown. The CSEM receiver positions are superimposed on this image. The inversion was for four frequencies of the inline and vertical electric and transverse magnetic fields.*

## 3D inversion of towed EM data

For 3D inversion of both towed EM and CSEM data, a common 3D earth model was used. That model consisted of a 110 m thick 0.3 ohm-m water column overlying an otherwise homogeneous half-space of 1.0 ohm-m. The 3D inversion domain was discretized to 9,000 cells of 200 m x 200 m x 100 m dimension. No a priori model was used, and the inversion itself was unconstrained.

Results of the 3D towed EM inversion are shown in Figure 5 (with survey lines superimposed). Results of the 3D CSEM inversion are shown in Figure 6 (with receiver positions superimposed). As one can see, there is much similarity between the results from the towed EM and CSEM inversions. For all intents and purposes, the results may be considered equivalent.

### Conclusions

We have introduced a practical methodology for 3D inversion of towed EM data based on a moving footprint. With 3D inversion of towed EM data simulated from a dynamic reservoir model, we have shown that the towed EM system can be used to detect and characterize the Harding field, which is a typical North Sea-type target. We have compared our 3D inversion of time-domain towed EM data with 3D inversion of conventional frequency-domain CSEM data. We observed similarities in the recovered models. Obviating the need for ocean bottom receivers, we note that the towed EM system enables CSEM data to be acquired simultaneously with seismic over very large areas in frontier and mature basins for higher production rates and relatively lower cost than conventional CSEM.

### Acknowledgements

The authors acknowledge TechnoImaging and PGS for support of this research and permission to publish. The Harding Central 3D resistivity models were developed as part of a research project H0531E between PGS, BP, and the UK Department of Trade and Industry (now Business, Innovation and Skills). BP and Maersk, as operators of the Harding field, are acknowledged for release of the Harding Central reservoir models.

**EDITED REFERENCES**

Note: This reference list is a copy-edited version of the reference list submitted by the author. Reference lists for the 2011 SEG Technical Program Expanded Abstracts have been copy edited so that references provided with the online metadata for each paper will achieve a high degree of linking to cited sources that appear on the Web.

**REFERENCES**

Cox, L. H., G. A. Wilson, and M. S. Zhdanov, 2010, 3D inversion of airborne electromagnetic data using a moving footprint: Exploration Geophysics, **41**, no. 4, 250–259, doi:10.1071/EG10003.

Hesthammer, J., A. Stefatos, M. Boulaenko, S. Fanavoll, and J. Danielsen, 2010, CSEM performance in light of well results: The Leading Edge, **29**, 34–41, doi:10.1190/1.3284051.

Hursán, G., and M. S. Zhdanov, 2002, Contraction integral equation method in three-dimensional electromagnetic modeling: Radio Science, **37**, no. 6, 1089, doi:10.1029/2001RS002513.

Mattsson, J. M., L. L. Lund, J. L. Lima, F. E. Englemark, and A. M. MacKay, 2010, Case study — A towed EM test at the Peon discovery in the North Sea: Presented at 72nd Annual International Conference and Exhibition, EAGE.

Ziolkowski, A., R. Parr, D. Wright, V. Nockles, C. Limond, E. Morris, and J. Linfoot, 2010, Multitransient electromagnetic repeatability experiment over the North Sea Harding field: Geophysical Prospecting, **58**, 1159–1176.

Zhdanov, M. S., 2002, Geophysical inverse theory and regularization problems, Elsevier.

Zhdanov, M. S., R. B. Smith, and A. Gribenko, M. Cuma, and M. Green, 2011, Three-dimensional inversion of large-scale EarthScope magnetotelluric data based on the integral equation method — Geoelectrical imaging of the Yellowstone conductive mantle plume: Geophysical Research Letters, **30**, L08307, doi: 10.1029/2011GL046953.

Zhdanov, M. S., E. P. Velikhov, M. Cuma, G. Wilson, N. Black, and A. Gribenko, 2010, Exploring multiple inversion scenarios for enhanced interpretation of CSEM data — An iterative migration analysis of the Shtokman gas field: First Break, **28**, 95–101.